

## Thermocapillary Effect of a Liquid Plug in Transient Temperature Fields

Nam-Trung NGUYEN\* and Xiaoyang HUANG

School of Mechanical and Production Engineering, Nanyang Technological University, 50 Nanyang Avenue, 639798 Singapore

(Received August 31, 2004; accepted October 23, 2004; published February 8, 2005)

In this paper we present the theoretical and experimental results of thermocapillary effects of liquid plugs in a long capillary, which is exposed to a transient temperature gradient. A one-dimensional analytical model is formulated for the dynamic behavior of a liquid droplet, which is driven by the thermocapillary effect under a transient temperature field. The thermocapillary actuation concept can be used for liquid transport in microfluidics. In microfluidic applications, the temperature field is often induced by the activation of integrated heaters. The generated temperature field and temperature gradient drive a liquid droplet according to the temperature-dependent surface tension. In the initial stage, the transient temperature gradient spreads in the capillary wall much slower than the droplet itself, and thus leads to an interesting behavior of droplet motion as described in this paper. Experiments were carried out for liquid droplets with different viscosities in long glass capillaries with different radii. The capillaries are exposed to a resistive heater at one of its ends. The analytically predicted behavior of the droplet motion agrees qualitatively well with the measurement. [DOI: 10.1143/JJAP.44.1139]

KEYWORDS: microfluidics, capillary, thermocapillary, surface tension, microdroplet, microplug

### 1. Introduction

Recently, microfluidics has been emerging as a key technology for biochemical analysis. Typical microfluidic applications utilize microdevices for liquid transport, mixing, separation, and chemical analysis. From many existing concepts, manipulation of microdroplets promises a huge potential in microfluidics. Pollack *et al.* proposed a droplet transport concept based on electrowetting, where surface tension is controlled by applied voltages.<sup>1)</sup> Another way of manipulating surface tension is utilizing the effect of thermocapillary. The temperature dependency of surface tension of a liquid/gas/solid system causes this effect. The viscosity and surface tension of a liquid decrease with increasing temperature. A gas bubble moves against the temperature gradient toward a higher temperature [Fig. 1(a)]. A liquid plug moves along the temperature gradient toward a lower temperature [Fig. 1(b)]. These phenomena are also called Marangoni effects. In practical applications, the temperature gradient can be generated using integrated heaters.

The motion of a droplet on a flat surface was previously investigated.<sup>2)</sup> Recently, this actuation concept found renewed interests from the microfluidics community.<sup>3,4)</sup> In these studies the dynamic behaviors of a droplet in a temperature field, such as the characteristics of droplet velocity versus its position, were examined. In addition to the simulation studies carried out by Darhuber *et al.* and Tseng *et al.*, no analytical theory was established for the

dynamic behavior of these droplets.<sup>3,4)</sup> In the past, a theory was reported for droplet motion caused by electrowetting.<sup>6)</sup> Heat transfer inside a thermocapillary droplet was studied by Sammarco and Burns.<sup>5)</sup> Yarin *et al.*<sup>7)</sup> reported a complex analytical model for the motion of droplets surrounding a thin fiber with a temperature gradient and a temperature jump as the initial conditions. However, to the best knowledge of the authors, no study was carried out on the dynamic behavior of a liquid plug inside a capillary under a transient temperature field. In this paper, we consider the one-dimensional model of a small liquid droplet in a cylindrical capillary. The model consists of two governing equations describing the spreading of thermal field in the capillary and the motion of the liquid plug.

### 2. Theory

#### 2.1 Transient temperature distribution in the capillary

At a relatively low heater temperature, heat radiation can be neglected. The energy equation for heat transport in the capillary wall can be formulated using heat conduction and free convection as

$$\frac{\partial T}{\partial t} = \alpha \frac{\partial^2 T}{\partial x^2} - \frac{2h}{\rho c R_0} T, \quad (1)$$

where  $T$  is the temperature difference compared to the ambient temperature,  $R_0$  is the outer diameter of the capillary,  $\alpha$ ,  $\rho$ , and  $c$  are the thermal diffusivity, density and specific heat capacity of the capillary material, respectively. The initial and boundary conditions of eq. (1) are

$$\begin{aligned} t = 0 : & \quad T(x) = 0 \\ t > 0 : & \quad \begin{cases} x = 0, & \frac{dT}{dx} = -q'/k \\ x = L_c, & T = 0, \end{cases} \end{aligned} \quad (2)$$

where  $L_c$ ,  $q'$ , and  $k$  are the length of the capillary and the heat flux and heat conductivity of capillary material, respectively. By introducing the dimensionless variables  $T^* = T/(q'L_c/k)$ ,  $x^* = x/L_c$ ,  $t^* = t/(L_c^2\alpha)$  and

$$\beta = \sqrt{\frac{hL_c^2}{kR_0}},$$

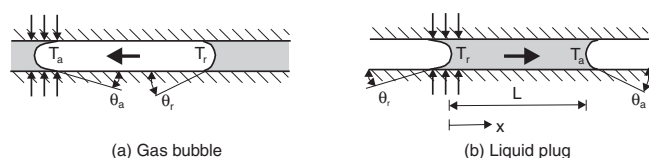


Fig. 1. Movement of a gas bubble (a) and a liquid plug (b) under the thermocapillary effect.

\*E-mail address: mntnguyen@ntu.edu.sg

where  $h = 0.631k_a/(2R_o)$  is the heat transfer coefficient on the outer capillary surface,<sup>7)</sup>  $k$ , the thermal conductivity of the capillary material, and  $k_a$ , the thermal conductivity of air, the dimensionless energy equation is expressed as:

$$\frac{\partial T^*}{\partial t^*} = \frac{\partial^2 T^*}{\partial x^{*2}} - \beta T^* \quad (3)$$

with the following dimensionless boundary conditions

$$\begin{aligned} t^* = 0: & \quad T^*(x^*) = 0 \\ t^* > 0: & \quad \begin{cases} x^* = 0, & \frac{dT^*}{dx^*} = -1 \\ x^* = 1, & T^* = 0, \end{cases} \end{aligned} \quad (4)$$

The solutions of the dimensionless temperature and temperature gradient are

$$\begin{aligned} T^* = & \frac{1}{\beta} \left[ \frac{\sinh(\beta)}{\cosh(\beta)} \cosh(\beta x^*) - \sinh(\beta x^*) \right] \\ & + \sum_{n=1}^{\infty} D_n \exp \left\{ - \left[ \left( n - \frac{1}{2} \right)^2 \pi^2 + \beta^2 \right] t^* \right\} \\ & \times \cos \left[ \left( n - \frac{1}{2} \right) \pi x^* \right] \end{aligned} \quad (5)$$

$$\begin{aligned} \frac{dT^*}{dx^*} = & \left[ \frac{\sinh(\beta)}{\cosh(\beta)} \sinh(\beta x^*) - \cosh(\beta x^*) \right] \\ & - \sum_{n=1}^{\infty} \left( n - \frac{1}{2} \right) D_n \exp \left\{ - \left[ \left( n - \frac{1}{2} \right)^2 \pi^2 + \beta^2 \right] t^* \right\} \\ & \times \sin \left[ \left( n - \frac{1}{2} \right) \pi x^* \right] \end{aligned} \quad (6)$$

with

$$\begin{aligned} D_n = & 2 \int_0^1 \left\{ - \frac{1}{\beta} \left[ \frac{\sinh(\beta)}{\cosh(\beta)} \cosh(\beta x^*) - \sinh(\beta x^*) \right] \right. \\ & \left. \times \cos \left[ \left( n - \frac{1}{2} \right) \pi x^* \right] dx^* \right\} \end{aligned} \quad (7)$$

Figure 2 depicts the typical dimensionless temperature and temperature gradient along the capillary.

## 2.2 Dynamic behavior of a liquid plug in a horizontal cylindrical capillary

Figure 1(b) shows the model of a liquid plug in a cylindrical capillary. The surface tension is a function of temperature, which in turn is a function of position  $x$  if a weak thermal interaction between the plug and the capillary can be assumed

$$\sigma_{lg}(T) = f[T(x)] = g(x) = \sigma_{lg}(x) \quad (8)$$

The simplest model for the friction between the liquid plug and the capillary wall is the Hagen-Poiseuille model:

$$\frac{dp}{dx} = \frac{8\mu}{R^2} \frac{dx}{dt}, \quad (9)$$

where  $R$  is the radius of the plug and  $\mu$  is the dynamic viscosity of the liquid. The force equilibrium of the liquid plug can be expressed as

$$\begin{aligned} \rho \pi R^2 L \frac{d^2 x}{dt^2} = & -8\pi \mu L \frac{dx}{dt} + 2\pi R [\sigma_{lg}(x+L) \cos \theta_a \\ & - \sigma_{lg}(x) \cos \theta_r], \end{aligned} \quad (10)$$

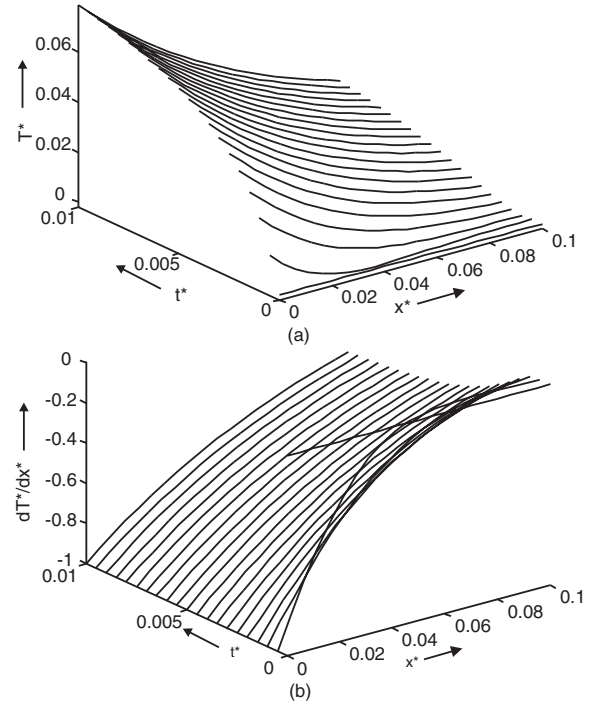


Fig. 2. Dimensionless analytical solution of (a) transient temperature distribution and (b) transient distribution of the temperature gradient along the capillary.

where  $L$ ,  $\theta_r$  and  $\theta_a$  are the length and contact angles at the receding and advancing ends of the liquid plug, respectively. By introducing the velocity  $u = dx/dt$ , rearranging (10) and introducing the kinetic viscosity  $\nu = \mu/\rho$ , the governing equation for the liquid plug is

$$\begin{aligned} \frac{du}{dt} + \left( \frac{8\nu}{R^2} \right) u + \frac{2}{\rho RL} [\sigma_{lg}(x+L) \cos \theta_a \\ - \sigma_{lg}(x) \cos \theta_r] = 0. \end{aligned} \quad (11)$$

The three terms on the left-hand side of the above equation represent the acceleration, the friction and the surface tension, respectively. For a small temperature range, the surface tension can be assumed as a linear function of temperature:

$$\sigma_{lg}(T) = \sigma_{lg0} - \gamma(T - T_0), \quad (12)$$

where  $\sigma_{lg0}$  is the surface tension at the reference temperature  $T_0$ . The temperature coefficient  $\gamma$  can be determined from the temperature function of the surface tension values.

The solution for the velocity  $u$  is:

$$u = \frac{B}{A} [1 - \exp(-At)]. \quad (13)$$

with:

$$A = \frac{8\nu}{R^2}, \quad B = \frac{2}{\rho RL} [-\sigma_{lg}(x) \cos \theta_r - \sigma_{lg}(x+L) \cos \theta_a],$$

The time, position, and velocity can be nondimensionalized according to the previous section using  $t^* = t/(L_c^2/\alpha)$ ,  $x^* = x/L_c$  and  $u^* = u/(L_c/\alpha)$ , respectively. The reference velocity  $u_0 = L_c/\alpha$  can be considered as the diffusion speed of the temperature. Assuming the same contact angle at the receding and advancing ends  $\theta$  and a short liquid plug  $L \ll L_c$ , the dimensionless form of (11) is

$$\frac{du^*}{dt^*} + \frac{8}{R^{*2}} \frac{\nu}{\alpha} u^* + \frac{2}{R^*} \frac{L^3 q'}{\rho k \alpha^2} \gamma \cos(\theta) \frac{dT^*}{dx^*} = 0, \quad (14)$$

The temperature gradient  $dT^*/dx^*$  is obtained using eq. (6). The solution for the dimensionless velocity  $u^*$  is

$$u^* = \frac{B^*}{A^*} [1 - \exp(-A^* t^*)] \quad (15)$$

with

$$A^* = \frac{8}{R^{*2}} \frac{\nu}{\alpha}, \quad B^* = \frac{2}{R^*} \frac{L^3 q'}{\rho k \alpha^2} \gamma \cos(\theta) \frac{dT^*}{dx^*},$$

where  $R^* = R/L_c$  is the dimensionless capillary radius. Based on eq. (15), the dynamic behavior of the liquid plug can be divided into two periods: the acceleration period and the stabilizing period. The acceleration period is determined by  $A^*$ , while the stabilizing period is determined by  $B^*$ . A less viscous plug will accelerate faster and reach a higher velocity initially. Since the liquid plug initially moves faster than the thermal diffusion, which is represented by  $L_c/\alpha$ , the velocity then decreases due to the lower temperature gradient.

### 3. Experiments

#### 3.1 Experimental setup

A measurement system was established for the observation of the dynamic behaviors of silicone oil plugs in a cylindrical capillary. The capillaries (Sigma-Aldrich) are made of glass and 14 cm long. Using a capillary wall thickness of 200  $\mu\text{m}$ , different inner radii of 1.26 mm, 1.55 mm, and 1.78 mm can be selected. One end of the capillaries is heated using a resistive wire. The resistive wire is made of nickel/chromium alloy (Ni80Cr20) (Goodfellow), which has a diameter of 125  $\mu\text{m}$ . The wire is insulated using a 8- $\mu\text{m}$ -thick polyimide layer. The heater consists of eight turns and is about 3 mm long. The capillary is suspended in a frame made of acrylic glass. The distance between the heater and the fixed end is  $L_c = 10$  cm. The motion of the plugs is captured using a digital CCD camera. The frame rate of the camera can be selected to suit the droplet speed. The image capturing process and the activation of the heater are synchronized using an external switch. The actual experimental setup is shown in Fig. 3.

Silicone oils, PDMS (polydimethylsiloxane, Sigma-Aldrich), were used as test liquids, which have different viscosities but almost the same surface tension. Three different oils,  $-\text{Si}(\text{CH}_3)_2\text{O}-$  ( $\nu = 10$  cSt,  $\rho = 930$  kg/m<sup>3</sup>),  $-\text{C}_7\text{H}_8\text{OSi}-$  ( $\nu = 100$  cSt,  $\rho = 960$  kg/m<sup>3</sup>) and  $-\text{Si}(\text{CH}_3)_2\text{O}-$  ( $\nu = 1000$  cSt,  $\rho = 970$  kg/m<sup>3</sup>), were used. The position of the droplet was evaluated frame by frame using a customized program written in MATLAB. The typical images of the captured frames are shown in Fig. 4.

#### 3.2 Experimental results and discussion

According to the actual experiments, an initial plug position of  $x_0^* = 0.005$  was used in the analytical results discussed in this section. The measured contact angle of 25° was also used in the analytical model. The results of the plug position versus time are depicted in Fig. 5. Figure 5(a) shows the theoretical position of liquid plugs at the same heat rate  $q'$  but with different viscosities of 10 cSt, 100 cSt,

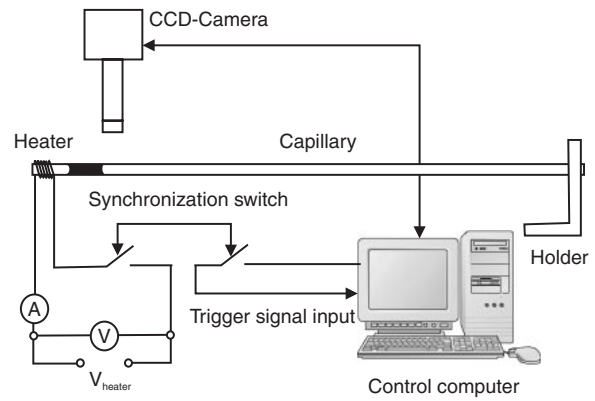


Fig. 3. Experimental setup for characterization of the dynamic behavior of a liquid plug in a capillary under a transient temperature field.

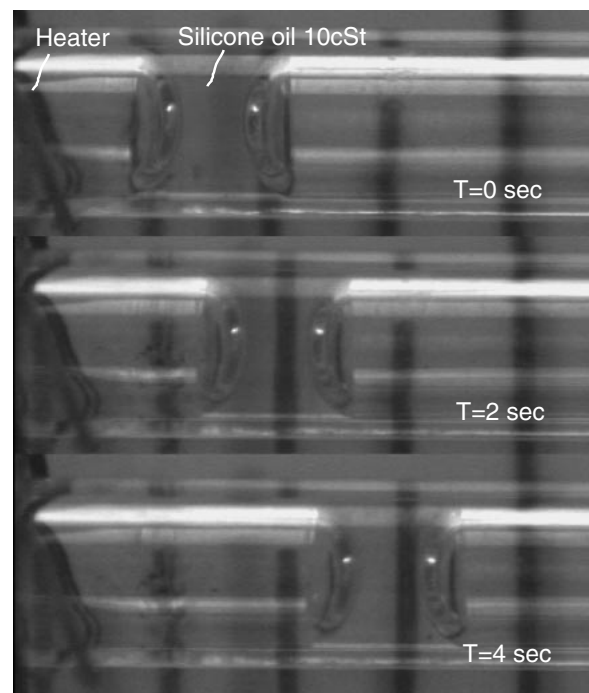


Fig. 4. Images of the captured frames after switching on the heater: (a)  $t = 0$  s, (b)  $t = 2$  s, and (c)  $t = 4$  s.

and 1000 cSt. The only fitting parameter is the heat rate  $q'$ . For the theoretical results, the properties of the glass capillary are assumed as  $\rho = 2500$  kg/m<sup>3</sup>,  $c = 750$  J/m<sup>3</sup>, and  $k = 1.4$  W/mK, while the thermal conductivity of air is assumed as  $k = 0.0261$  W/mK. The dynamic behavior of the plugs can be seen clearly in Fig. 6, which depicts the theoretical and experimental results of velocities versus positions. The measured velocities were evaluated based on the original data of the position-versus-time measurement depicted in Fig. 5(b).

The two periods of the initial behavior can be observed clearly in Fig. 6. After an acceleration period, the liquid plug decelerates due to the lower temperature gradient. The acceleration period is determined by  $A^*$  in eq. (15) or the ratio  $\nu/\alpha$  between the kinematic viscosity (momentum diffusivity) of the liquid and the thermal diffusivity of the capillary material. The stabilizing period is determined by  $B^*$  or the heat transfer in the capillary wall as modeled in

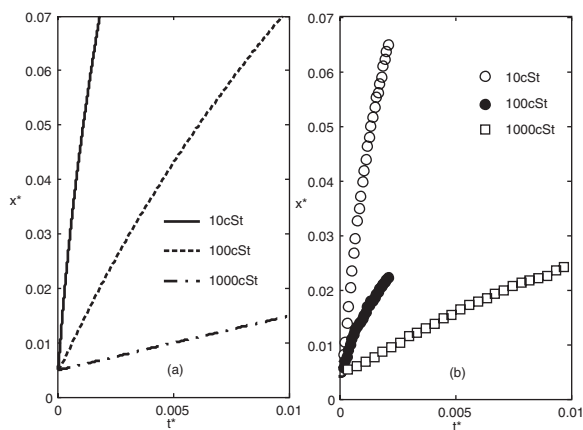


Fig. 5. Position of liquid plugs with different viscosities after switching on the heater ( $t^* \geq 0$ ): (a) theoretical results, and (b) experimental results. The data points are measured results. The lines are fitting functions based on the presented analytical model (initial position:  $x_0 = 0.5$  mm; properties of the glass capillary:  $\rho = 2500$  kg/m<sup>3</sup>,  $c = 750$  J/m<sup>3</sup>, and  $k = 1.4$  W/mK; property of air:  $k = 0.0261$  W/mK). The only fitting parameter is the heat flux  $q' = 909.5$  W/m<sup>2</sup>, which was chosen for the droplet with a viscosity of 10 cSt. The same heat flux is applied to droplets with viscosities of 100 cSt and 1000 cSt.

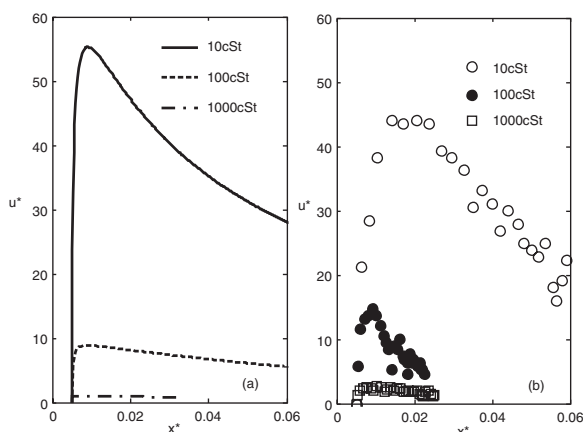


Fig. 6. Velocity of liquid plugs with different viscosities at different positions: (a) theoretical results, and (b) experimental results (the same conditions as those in Fig. 5 apply).

eq. (3). A less viscous drop accelerates faster and reaches a higher velocity initially. The velocity then decreases and approaches the steady state condition.

A smaller capillary radius  $R^*$  leads to a higher  $B^*$  in eq. (15), and thus a higher velocity. Although  $v/\alpha$  in  $A^*$  and  $R^*$  in  $B^*$  have the same order of influence on the velocity, the difference caused by  $v/\alpha$  can be observed clearly because of the 2 and 3 orders of the difference in viscosity. In the case of the capillaries used in our experiments, radii have the same size order, thus the difference caused by the capillary radius is not apparent in Figs. 7 and 8.

#### 4. Conclusions

We have reported a simple analytical model for the transient behavior of a liquid plug in a cylindrical capillary, which is subjected to a transient temperature field. The initial condition of the temperature field exists in many practical microfluidic devices for the manipulation of

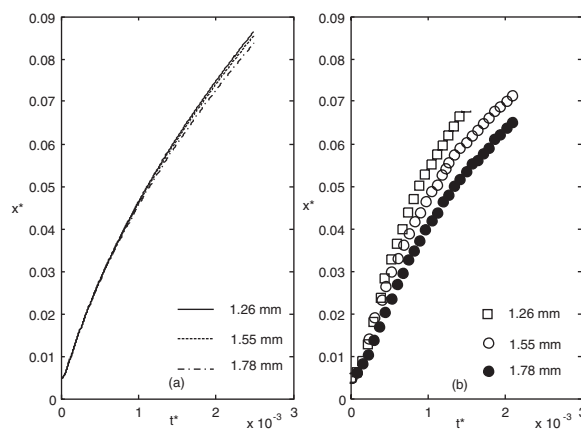


Fig. 7. Position of liquid plugs with different capillary radii after switching on the heater ( $t^* \geq 0$ ): (a) theoretical results, and (b) experimental results (the same conditions as those in Fig. 5 apply).

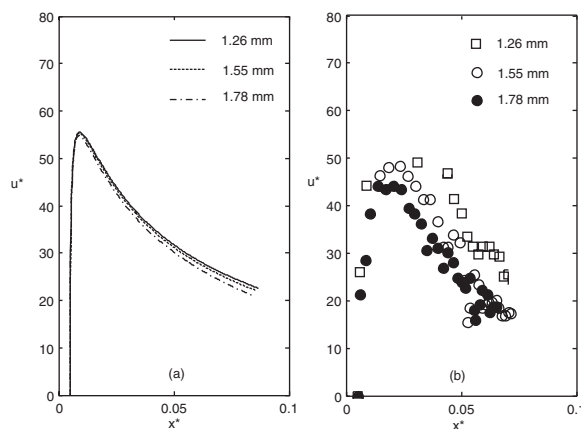


Fig. 8. Velocity of liquid plugs with different capillary radii at different positions: (a) theoretical results, and (b) experimental results (the same conditions of Fig. 5 apply).

droplets using thermocapillary effects. A liquid plug in a capillary first accelerates to a maximum velocity under the influence of the temperature gradient near a heater after switching it on. Because the thermal diffusivity is lower than the initial velocity of the plug, the plug moves out of the high-gradient region and decelerates. The predicted behavior agrees qualitatively well with the measured results. The model can be further improved using the lubrication theory for the friction term in eq. (9) and a temperature-dependent viscosity. This model can serve as a tool for designing microheaters and heating sequences for microfluidic actuation by the modulation of surface tension.<sup>3)</sup>

- 1) M. G. Pollack, R. B. Fair and A. D. Shenderov: Appl. Phys. Lett. **77** (2000) 1725.
- 2) J. B. Brozoska, F. Brochard-Wyart and F. Rondelez: Langmuir **9** (1993) 2220.
- 3) A. A. Darhuber, J. P. Valentino, J. M. Davis and S. M. Troian: Appl. Phys. Lett. **82** (2003) 657.
- 4) Y. T. Tseng, F. G. Tseng, Y. F. Cheng and C. C. Chieng: Sens. Actuat. A **114** (2004) 292.
- 5) H. R. Ren, B. Fair, M. G. Pollack and R. J. Shaughnessy: Sens. Actuat. B **91** (2002) 201.
- 6) T. S. Sammarco and M. A. Burns: J. Micromech. Microeng. **10** (2000) 42.
- 7) A. L. Yarin, W. Liu and D. H. Reneker: J. Appl. Phys. **91** (2002) 4751.